Iğdır Üniversitesi Fen Bilimleri Enstitüsü Dergisi, 15(2), 658-674, 2025
Journal of the Institute of Science and Technology, 15(2), 658-674, 2025

ISSN: 2146-0574, eISSN: 2536-4618

Mechanical Engineering **DOI: 10.21597/jist.1583576**

Research Article

Received: 12.11.2024 **Accepted: 17.12.2024**

To Cite: Dikmetaş, C.M., Mıtıncık, S., Aktürk A. & Yazıcı, M.Y. (2025). Numerical Modelling of Graphite-Based Composite Thermal Energy Storage Unit: Effect of Numerical Variables. *Journal of the Institute of Science and Technology*, 15(2), 658-674.

Numerical Modelling of Graphite-Based Composite Thermal Energy Storage Unit: Effect of Numerical Variable

Celal Mert DİKMETAŞ[1], Sare MITINCIK[1], Ahmet AKTÜRK[2*], Mustafa Yusuf YAZICI[1]

Highlights:

- Numerical variables
- Liquid fraction
- Energy storage rate
- Temperature variation

Keywords:

- Latent heat thermal energy storage
- Paraffin
- Graphite
- Phase change
- Enthalpy-Porosity technique

ABSTRACT:

Thermal energy storage (TES) systems have a great potential on the providing balance of energy demand/supply, while also contributing to net-zero emissions, a reduced carbon footprint, and a greener environment. Paraffin phase change materials have emerged as a prominent material for TES applications due to its potentially high energy storage density. However, their application is significantly limited by its low thermal conductivity values. This study introduces a composite structure for thermal energy storage, utilizing paraffin as the latent heat storage material and a graphite matrix to enhance thermal conductivity for solar energy and waste heat applications. The effects of various numerical variables of mushy zone parameter, the pressure-velocity coupling, the pressure discretization scheme, and the boundary condition on the melting performance of a PCM-based thermal energy storage system were investigated within an annular storage medium, extending beyond the literature. Simulations were performed using ANSYS-Fluent, employing the enthalpy-porosity technique. The validation of the study was ensured based on the experimental setup. The primary aim of the study was to identify the numerical variables that yield the most realistic results. It was found that most closely representation of the experimental/real conditions is 10^5 mushy zone constant, a Coupled algorithm for the pressure-velocity coupling, and PRESTO! for the pressure discretization scheme. However, numerical variable effect was not significantly notable for the paraffin-impregnated graphite matrix storage medium. Results also indicated that graphite constrained the motion of paraffin, resulting in a uniform and homogeneous temperature distribution. It is observed that differences in numerical parameters lead to variations (0.42-16.57%) in energy storage rates, considering melting/charging times and the final temperatures of the TES system.

1 Celal Mert DİKMETAŞ (**Orcid ID**: 0009-0009-7635-3498), Sare MITINCIK (**Orcid ID:** 0000-0003-0149-8990),Mustafa Yusuf YAZICI (**Orcid ID:** 0000-0002-1076-9265), Samsun University, Faculty of Engineering and Natural Sciences, Department of Mechanical Engineering, Samsun, Türkiye
[2] Ahmet AKTÜRK (**Orcid ID:** 0000-0002-2985-2560), Iğdır University, Faculty of Engineering, Department of Mechanical Engineering, Iğdır, Türkiye

***Sorumlu Yazar/*Corresponding Author*:** Ahmet AKTÜRK, e-mail: aakturk@igdir.edu.tr

INTRODUCTION

Latent heat thermal energy storage system is one of the key technologies for energy conservation and offers a remarkable solution by providing a balance between energy supply and demand (Dinçer & Rosen, 2002), (Singh et al., 2023). The utilization of latent heat thermal energy storage employing phase change materials (PCMs) has the potential to provide substantial quantities of thermal energy storage, principally due to their considerable energy storage density, which is achieved through a nearly constant temperature/isothermal phase change (Chinnasamy et al., 2023). However, a main drawback of PCMs is their inheritly low thermal conductivity (0.1-0.3 W/mK) (Tong et al., 2019), (Nair et al., 2023). Minimizing the heat flow resistance by improving the thermal conductivity of PCMs and thus increasing heat transfer rates leads to a significant reduction in charge/discharge times in storage systems. To achieve this, a number of techniques may be employed, including the use of a metal matrix (Buonomo et al., 2019; Pourakabar et al., 2019), expanded graphite (Chakraborty et al., 2022; Elakkiyadasan et al., 2022), graphene (Cai et al., 2021; Feng et al., 2020), micro/nano encapsulation (Cano et al., 2016), nanoparticle addition (Khatibi et al., 2021), or graphite foam (Opolot et al., 2020). Among the present approaches, expanded graphite is an important candidate for overcoming the low thermal conductivity of PCMs, thanks to its excellent thermal properties, including low density (leads to increased PCM absorption), high porosity (over 80%), good adsorption performance, large surface area, chemical stability and high thermal conductivity (Liu.et al., 2022; Mitali et al., 2022; Yazici, 2022). In this sense, the graphite material enables the rapid flow/diffusion of heat through the thermal conductivity framework within the composite structure by enabling the formation of highly conductive heat conduction channels and significantly reducing the interfacial thermal resistance (Liu.et al., 2022), (Muraleedharan Nair et al., 2024).

Thermal conductivity enhancement studies in the literature for latent heat thermal energy storage systems by adding graphite material to PCM are presented in below. Song et al. (2019) conducted an experimental and numerical investigation into a series of samples with the objective of achieving a zero-leakage and high thermal conductivity by modifying the quantity of graphite within the dodecane/graphite composite structure. Melting and solidification processes were considered separately in a shell-in-tube geometry, and it was observed that the ideal amount of graphite in the composite structure was 16%. Furthermore, the thermal conductivity value of the composite structure increased 15 times with the addition of graphite compared to the pure dodecane case. Wu et al. (2020) carried out experimental and numerical investigations into the storage process of a ternary composite structure composed of paraffin, expanded graphite and nanocopper for passive solar heating. The results demonstrated that the porosity of graphite constrains the agglomeration of copper, and the incorporation of graphite enhances the heat storage process by elevating the thermal conductivity value to a degree that is 9.5 times greater than that observed in the pure paraffin case. On the other hand, the incorporation of copper markedly accelerated the phase change process of the composite PCM, resulting in a 152.17% increase in storage rates and a 100% increment in recovery rates. Mhiri et al. (2020) embedded the PCM/graphite nanocomposite structure, developed with the objective of enhancing the thermal conductivity of RT60 storage media, into carbon foam with the aim of limiting supercooling during melting process. The thermal behavior of the produced material was investigated through both experimental and numerical. Results demonstrated that the incorporation of the nanocomposite and carbon foam enhanced the melting process by 42%, while simultaneously increasing the thermal conductivity of pure RT60 by 9 times. Fteiti et al. (2020) has numerically investigated the thermal energy storage and recovery performance of octadecane-phase change material-in the melting and solidification

process by embedding it in a high thermal conductivity graphite matrix. The authors found that increasing the thermal conductivity value increases the melting/storage and solidification/recovery rates of the PCM. In addition, it was concluded that after the melting process is complete, the sensible heat storage that occurs while the heat source is still applied delays solidification and reduces the amount of latent heat storage. Zhao et al. (2021) numerically investigated the thermal energy storage and recovery processes of PCM581+graphite foam composites at different foam porosities and different filler configurations. The results showed that the graphite foam with 0.9% porosity had the best thermal performance (41.6% of the pure paraffin case for melting time and 7.6% of the pure paraffin case for solidification time). It was also found that the graphite foam placed only at the base of the storage geometry accelerated the melting process and deteriorated the solidification process. Li et al. (2022) numerically investigated four different performance enhancement methods (topology optimized fin, metal foam, longitudinal fin, shape-stabilized composite PCM) in an annular geometry. The results showed that the melting process was reduced by 88%, 86%, 84% and 83%, respectively. Mitincik & Yazici (2023) numerically analyzed (with experimental validation) the effect of composite bulk density (0, 23, 50, 100 and 143 kg/m^3) and wall temperature in a paraffin-impregnated graphite matrix material in a shell-in-tube geometry. The results showed that the increase in bulk density enhanced the charging performance by 76 times, but the alteration in performance was limited to 8% when the optimum bulk density (100kg/m^3) was exceeded. It was also observed that the wall temperature effect was greater at lower composite bulk densities due to the change in thermophysical properties. Mitincik & Yazici (2024) evaluated the performance of paraffin-impregnated graphite matrix structures with five different bulk densities of 0, 23, 50, 100 and 143 kg/m³ in thermal energy storage applications. In the experimentally validated numerical study, which was investigated at wall temperatures of 15, 25, 35 and 45°C, corresponding to real applications such as domestic water, power plant waste heat and geothermal energy, it was observed that increasing the density of composite improves the solidification behavior by forming a conduction heat transfer chain in the structure. Furthermore, study also showed that low wall temperatures offer higher discharging performance. Kumar et al. (2024) numerically and experimentally compared pure PCM (paraffin) and composite PCM (paraffin+graphite) for latent heat thermal energy storage. They investigated the effect of the composite material on melting/charging dynamics, and found that the composite PCM exhibited significantly improved thermal conductivity, temperature uniformity and prevented potential hot spots. They also defined a new parameter called Melt Time Ratio (MTR) and compared the improved heat transfer rate obtained by free convection (natural convection) with the improved heat transfer rate obtained by the addition of Compressed Expanded Graphite (CEG). It was found that rapid melting is prevented when the CEG is above or below a certain volume fraction.

This study presents a comprehensive numerical investigation of a phase change material-embedded graphite matrix (PCM/graphite matrix) thermal energy storage medium with a bulk density of 75 kg/m³ in annular geometry for solar energy and waste heat applications, considering sustainable and green energy applications. The novelty of this work is that the effect of numerical variables is investigated for the first time by the authors' best knowledge considering the limited number of numerical studies in the literature where a phase change material is embedded in graphite structure. Mushy zone constant (10^5,10^6,10^7,10^8), pressure-velocity coupling (SIMPLE, SIMPLEC, PISO, Coupled), pressure discretization schemes (PRESTO!, Body Force Weighted), and boundary conditions (isothermal wall, adiabatic) has evaluated through Computational Fluid Dynamics (CFD) software ANSYS-Fluent package program and compared using data from the experimental setup. The primary objective of this investigation is to determine the numerical variables that most closely approximate the characteristics of the real system. In this sense, it is aimed to obtain new insights by establishing a

reference point for the future studies. It should be noted that the numerical model plays a significant role in reducing the costs of the experimental set-up. Evaluation of the melting/storage analysis was based on time-dependent temperature profiles of the thermal energy storage media and the liquid fraction, as well as energy storage rate for performance assessment of storage medium.

MATERIALS AND METHODS

Experimental Procedure

In order to validate the numerical model and to establish a reference for the numerical studies, the experimental setup, which has been previously examined in detail by Mitincik & Yazici (2023) was taken as a basis. The graphite matrix structure impregnated with a phase change material (paraffin) was subjected to three processes: (1) heating of expandable graphite to obtain expanded graphite powder, (2) compaction of expanded graphite powders in a uniaxial mold, and (3) absorption of paraffin into graphite pores by capillarity effect and surface forces in a vacuum condition. The paraffin-impregnated PCM/graphite matrix block (composite block), and test section are displayed in Figure 1. The composite block with a 90/10 paraffin/graphite matrix mass ratio has a bulk density of 75 kg/m^3 and its properties are presented in Table 1. Although the bulk density varies with the applied compressive force (set at 80N for this study), literature suggests that achieving bulk densities above 150 kg/m³ is not advisable This is due to the fact that increased bulk density tends to close the pores, thereby reducing the absorption of paraffin-which facilitates thermal energy storage-and consequently diminishing the storage capacity. The use of PCM/graphite matrix with a density of 75 kg/m³ ensures high thermal conductivity in the storage medium while also striving to maintain the thermal storage capacity of the phase change material as high as possible. The graphite material with its low density, robust physical and chemical structure, high pore ratios and excellent thermal conductivity, stimulated the molecular chains of the paraffin, forming a thermal conduction path in the structure and increasing the thermal conductivity of the storage medium by approximately 35 times (Yazici et al., 2021).

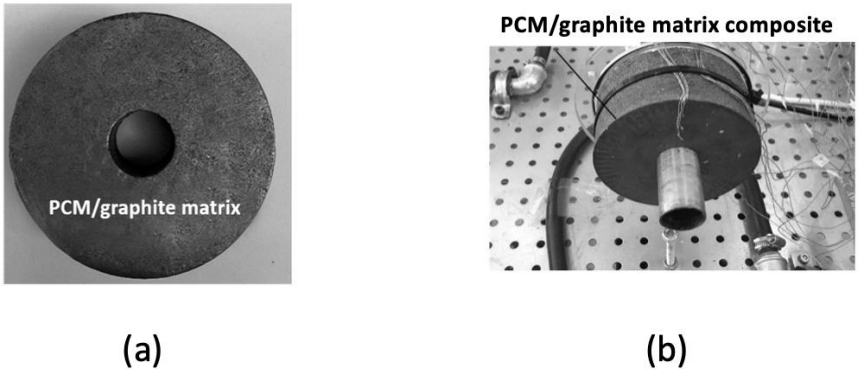

Figure 1. PCM/graphite matrix block (a), and test section (b)

Table 1. Thermo-physical properties of paraffin and paraffin/graphite composite material

Property	Paraffin	Paraffin/graphite composite material
Density (kg/m^3)	854 (< ±0.2)	773
Specific heat (J/kgK)	1540 (< ±1)	1400
Thermal conductivity (W/mK)	0.21 (< ±5)	7
Viscosity (Ns/m^2)	0.00003 (< ±1)	100000
Latent heat (J/kg)	165000 (< ±1)	147000
Solidus Temperature (°C)	49 (< ±0.1)	48
Liquidus Temperature (°C)	56 (< ±0.1)	56

Numerical Procedure

In the ANSYS Fluent, phase change problems are solved by a finite volume approach utilizing the enthalpy-porosity technique. This technique, developed by Voller & Prakash (1987) defines enthalpy as a temperature-dependent variable. Consequently, the energy equation is applicable to both regions (solid, liquid) and interfaces (porous region) (Brent et al., 1988).

Physical model

The investigation of phase change material (paraffin) embedded with graphite matrix composite thermal energy storage media was evaluated using the numerical model depicted in Figure 2, with experimental validation. Since the length of the storage medium manufactured by authors in experimental study (Mitincik & Yazici, 2023; Mitincik & Yazici, 2024) was 50 mm, the problem was analyzed by neglecting the effect of the heat transfer fluid in the flow direction and by considering the problem in 2-D. The right side of the calculation area is taken due to the mirror symmetry in the annular storage medium with simplified geometrical dimensions of 28.5mm (inner diameter)-113.8mm (outer diameter), neglecting the inner and outer pipe thicknesses. It results in diminished time required for the calculations. In the simulations, the initial temperature of the storage medium and the ambient temperature were set at 25°C. An isothermal wall boundary condition of 76°C was applied to the inner surface of the geometry, representing the hot heat transfer fluid. This temperature value is based on the mean temperature of the thermocouples located on the surface of the heat transfer pipe in the experimental study (Mitincik & Yazici, 2023). A convection heat transfer coefficient value of 3 W/m²K was defined on the outer surface of the geometry, taking into account the range of heat loss to the surrounding environment in still air (0-25 W/m²K). The distances of the local points positioned for temperature readings from the isothermal wall were 10 mm, 20 mm, 30 mm and 35 mm, respectively.

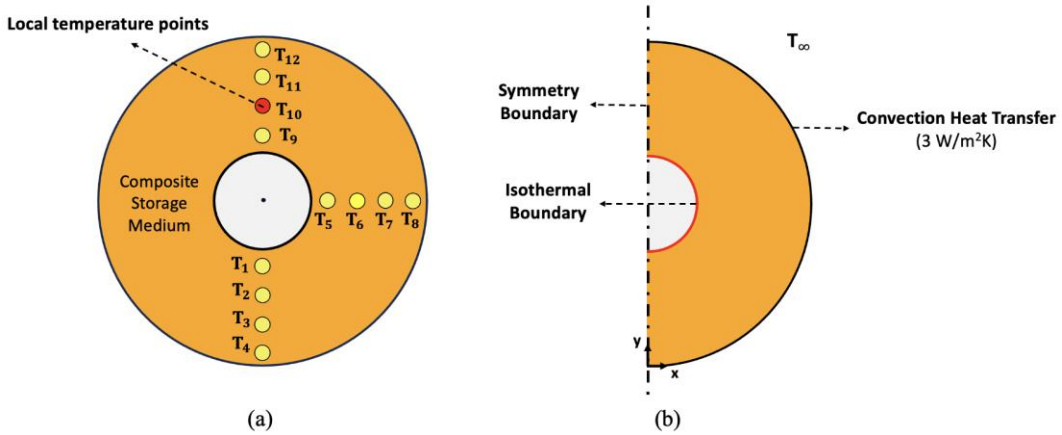

Figure 2. Local temperature points (a), schematic representation of model design for numerical studies (b)

Assumptions

The assumptions made for the numerical study are as follows:

- The liquid phase change material (PCM) is Newtonian, laminar and incompressible.
- The composite structure is homogeneous and isotropic.
- The thermophysical properties of the composite PCM are assumed to be independent of temperature.
- Volumetric expansion in the PCM during the phase change process is neglected.
- The density changes of the composite material during the phase change are negligible and heat transfer is only by conduction.
- Since there is no fluid movement in the composite structure, the viscosity is assumed to be very high (10^5) (Ling et al., 2015; Zhao et al., 2016).

Governing equations

The governing equations for the established 2-D numerical model are as follows:

Continuity Equation

$$\frac{\partial u}{\partial x}+\frac{\partial v}{\partial y}=0 \tag{1}$$

Momentum Equation

x direction:

$$\frac{\partial(\rho u)}{\partial(t)}+\frac{\partial(\rho uu)}{\partial x}+\frac{\partial(\rho vu)}{\partial y}=\frac{\partial}{\partial x}\left(\mu\frac{\partial u}{\partial x}\right)+\frac{\partial}{\partial y}\left(\mu\frac{\partial u}{\partial y}\right)-\frac{\partial P}{\partial x}+A_s u \tag{2}$$

y direction:

$$\frac{\partial(\rho v)}{\partial(t)}+\frac{\partial(\rho uv)}{\partial x}+\frac{\partial(\rho vv)}{\partial y}=\frac{\partial}{\partial x}\left(\mu\frac{\partial v}{\partial x}\right)+\frac{\partial}{\partial y}\left(\mu\frac{\partial v}{\partial y}\right)-\frac{\partial P}{\partial y}+A_s v \tag{3}$$

A correction term is added to the Navier-Stokes equations for melting and solidification problems (ANSYS Inc, 2013). It serves to suppress the velocity of the PCM when it is solid or mushy, and is shown as follows:

$$A_s=-C\frac{(1-\lambda)^2}{\lambda^3+\varepsilon} \tag{4}$$

The constant C, which denotes the 'mushy region', is among the variables subjected to numerical investigation in this study. For the coefficient within the range of 10^3 to 10^8, detailed information can be found in the relevant section (see Section 4.2). ε is a small value of 0.001 to prevent the expression from becoming 0, ensuring the phase change of the PCM is continuously included in the calculation (ANSYS Inc, 2013).

Energy Equation:

$$\frac{\partial(\rho H)}{\partial(t)}+\frac{\partial(\rho uH)}{\partial x}+\frac{\partial(\rho vH)}{\partial y}=\frac{\partial}{\partial x}\left(k\frac{\partial T}{\partial x}\right)+\frac{\partial}{\partial y}\left(k\frac{\partial T}{\partial y}\right) \tag{5}$$

The term "H" represents the total enthalpy, which is the sum of the sensible and latent heat, and its representation is as follows:

$$H=h+\Delta H \tag{6}$$

$$h=h_0+\int_{T_0}^{T}c_p dT \tag{7}$$

$$\Delta H=\lambda L \tag{8}$$

Here, L represents the latent heat, and λ denotes the liquid fraction, and the volume-weighted average method is employed to calculate melting. λ varies according to the relationship given below, and it is equal to zero in the case of a completely solid region.

$$\lambda = \begin{cases} 0 & T < T_{solidification} \\ \dfrac{T - T_{solidification}}{T_{melting} - T_{solidification}} & T_{solidification} < T < T_{melting} \\ 1 & T > T_{melting} \end{cases} \quad (9)$$

Solution independency and model validation

Before the numerical simulations, it is essential to demonstrate that the solutions are independent of the mesh/grid and time step. Results of the studies on mesh and time step independency, which were conducted with pure paraffin as a reference case, are presented in Figure 3 and Tables 2 in below and in graphical form at Mitincik & Yazici (2023) and Mitincik & Yazici, 2024. The numerical study employs different grid sizes of 19200, 27000, and 39600, along with time steps of 0.5, 1, and 2 seconds. Since no significant changes were observed after 27000 cell numbers and 1sec time step value in the independency studies considering liquid fraction, these values were taken as a basis for further numerical studies. Furthermore, it should be emphasized that a structural mesh was applied and a fine mesh was adopted due to the high temperature and density gradients near the isothermal wall.

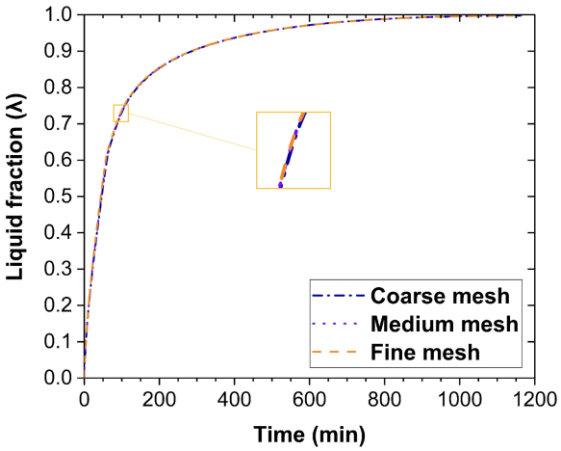

Figure 3. Mesh independency study based on liquid fraction (λ)

Table 2. Liquid fraction (λ) at different time steps and various time durations

	30min	150min	300min	1200min
0.5sec	0.344	0.851	0.904	1.0
1sec	0.347	0.856	0.905	1.0
2sec	0.349	0.857	0.907	1.0

On the other hand, the reliability of the established model is largely based on the model validation. As previously stated in Section 2 (Experimental Procedure), the present model validation is based on the temperature data obtained through the experimental setup. The total error in the temperature measurements obtained from the thermocouples was determined to be ±1.25%, attributed to the equipment, using the Kline and McClintock method. Figure 4 depicts the model validation plot considering the time-dependent T_{10} local point temperature profile of the composite with a bulk density of 75 kg/m³. It is observed that there is a minor deviation between the present model and the experimental result. This discrepancy is directly related to the thermophysical properties of the material used in the model, including the melting temperature and specific heat. Although the properties of composite PCM exhibit a temperature dependent character in reality, all thermophysical properties are considered to be independent of temperature in the numerical study (see assumptions). Therefore, it is concluded that the overall temperature profiles are reasonably consistent and reliable for modeling the composite storage medium.

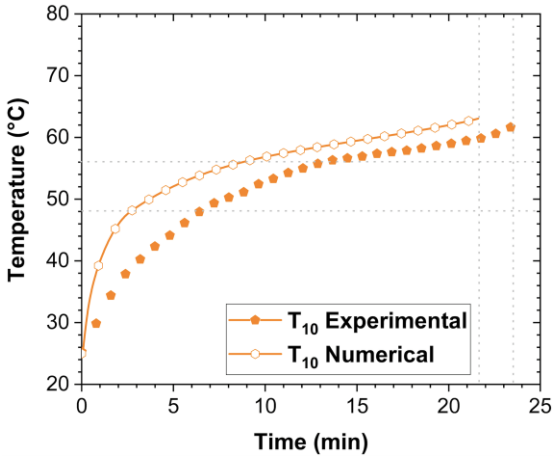

Figure 4. Numerical model validation for composite PCM with the local point temperature profile of T_{10}

RESULTS AND DISCUSSION

In the phase change thermal energy storage process, paraffin has been a material that attracts attention with significant advantages (high storage density, wide melting range, small volume change, corrosiveness). In addition, graphite material, which serves as a matrix structure and in which paraffin is embedded/encapsulated, is an optimal material for minimizing the low thermal conductivity and leakage issues of paraffin. This is due to its low density, high pore ratio, high heat transfer surface/volume ratio, and high thermal conductivity, which are inherent properties of the material. In this study, a numerical variable analysis has conducted on a paraffin/graphite matrix composite thermal energy storage medium with a bulk density of 75 kg/m^3. The numerical variables investigated are as follows: Mushy zone constant (10^5, 10^6, 10^7, 10^8), pressure-velocity coupling (SIMPLE, SIMPLEC, PISO, Coupled), pressure discretization schemes (PRESTO!, Body Force Weighted) and boundary conditions (isothermal wall, adiabatic wall). The analyses were conducted using ANSYS-Fluent, a computational fluid dynamics (CFD) software package. The main objective of the study is to determine the numerical variables that give the most realistic/appropriate results. In addition, a performance evaluation of all cases is made depending on the amount of energy stored, storage mass and melting/charging/storage times. It presents a comprehensive assessment of the numerical findings for the paraffin/graphite matrix storage media.

Evaluation of Temperature Uniformity in Storage Medium

Figure 5 illustrates the time-dependent temperature profiles of the numerical model for a paraffin impregnated graphite matrix composite storage medium with a bulk density of 75 kg/m³ at local points positioning at the lower, middle, and upper of the geometry. The horizontal dashed lines show the melting/phase change temperature range of the composite structure (48-56°C), while the vertical dashed lines represent the sensible energy (<40sec), latent energy (40-1081sec) and second sensible energy (>1081s) storage processes, respectively. The graphite matrix with a microporous structure act as a physical barrier, preventing the natural convection effect and allowing the liquid paraffin to be retained. This results in a uniform temperature distribution and, consequently, a uniform melting characteristic within the storage medium, as illustrated in Figure 5. For instance, temperature values recorded at points T_2, T_6 and T_{10} at t=400s are 54°C, 54°C, and 54°C, respectively. Results provides clear evidence that the effective heat transfer mechanism in the paraffin/graphite matrix storage medium is by conduction. It should be noted that natural convection heat transfer does not occur in pore sizes/diameters of less than 10 mm (Kang et al., 2019). Accordingly, only one local point (T_{10}) is analyzed for temperature in the numerical variable analysis that follows. It can be observed that the temperature increase rates are

generally faster up to the phase transition point (48°C). Upon reaching the phase transformation point, the local temperature increasing rates decline (40-1081sec). Subsequently, the local point temperatures exhibit a rapid increase upon completion of the phase transformation period in the following period (after 1031sec). On the other hand, a drop in temperature readings is observed as a result of the decrease in thermal gradients with radial distance from the heat source. To illustrate, the temperature readings for points T_5, T_6, T_7, and T_8 at t=600 sec are 65°C, 56°C, 51°C, and 50°C, respectively.

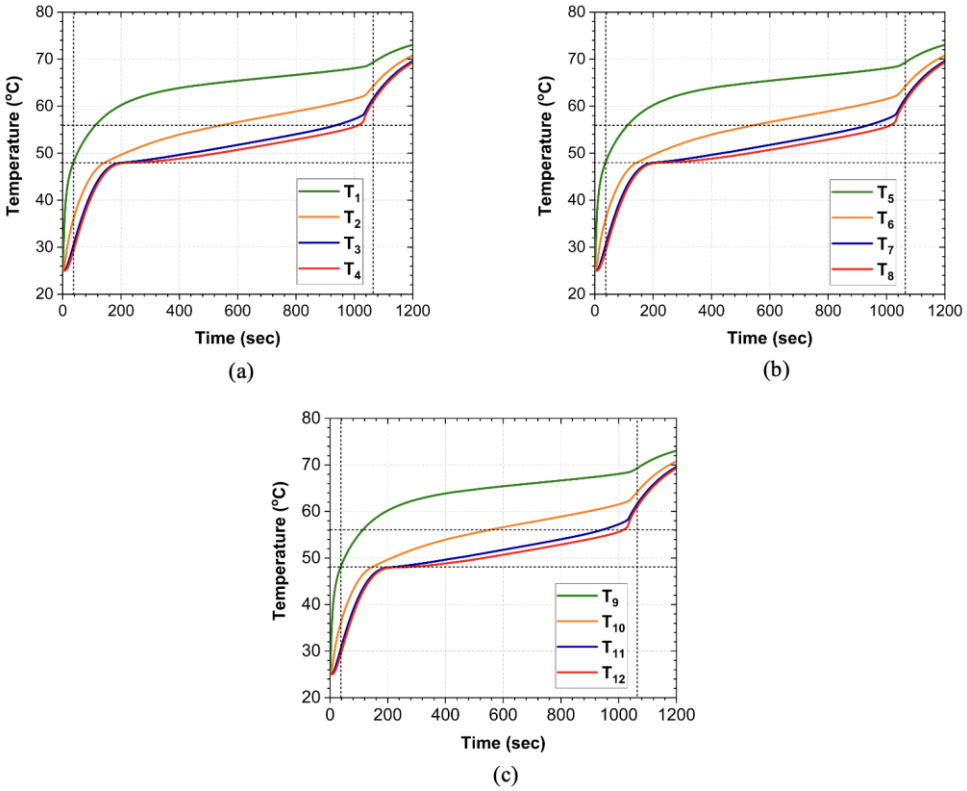

Figure 5. Local temperature variations in the lower (a), middle (b), and upper (c) regions for the numerical model with a paraffin/graphite matrix storage medium of 75 kg/m³ bulk density

Effect of Mushy Zone Parameter

The mushy zone constant (C) is a critical parameter that defines the region where liquid and solid phases simultaneously exist in phase change process. In this region, the fluidity and heat transfer of the material are determined by their interaction. Consequently, the temperature distribution within the storage medium and liquid fraction are affected. Identifying an appropriate value for the mushy zone constant, defined within the range of 10^5 to 10^8, is crucial for understanding the dynamics of melting and solidification, as well as the associated thermal-fluid behavior. This is because the parameter determines the density of the mushy zone and the nature of the phase transition (Versteeg & Malalasekera, 2007; Tu et al., 2018). Figure 6 illustrates the local point temperature profiles at T_{10} in the numerical and experimental studies (a) and the liquid fraction contours at t=600s (b) for varying mushy zone constants. It was determined that the mushy constant yielding the most accurate results in alignment with the experimental findings was 10^5 with 1031sec melting time. It can be readily concluded that the mushy zone constant has a direct impact on the transfer of thermal energy, and thus on the thermal energy storage process. For example, it is seen that the temperature readings of 10^5, 10^6, 10^7, and 10^8 mushy zone constants for t=600sec are 56°C, 57.5°C, 56°C, 56°C, 56°C, respectively. It is observed that the temperature at T_{10} in the experimental case at t=600sec is 52°C. It is also supported by the melting times. The completion of the storage/melting process for the 10^5, 10^6, 10^7, and 10^8 mushy zone constants is achieved in 1031sec, 881sec, 1027sec, and 1027sec, respectively. It should be noted that this period

of time was 1410s in experimental procedure. On the other hand, it can be seen that at t=600s the phase interface moves faster and the melt front expands as melting accelerates with increasing values of the mushy zone constant (C). To illustrate, in the case of the 10^6 mushy zone constant, where the numerical simulation is completed at the earliest, the melting interface progresses at a faster rate than other mushy zone constants. At the same time, it can be seen that there is a thin mushy zone since the temperature gradients decrease due to the increased thermal conductivity with graphite material in the storage medium.

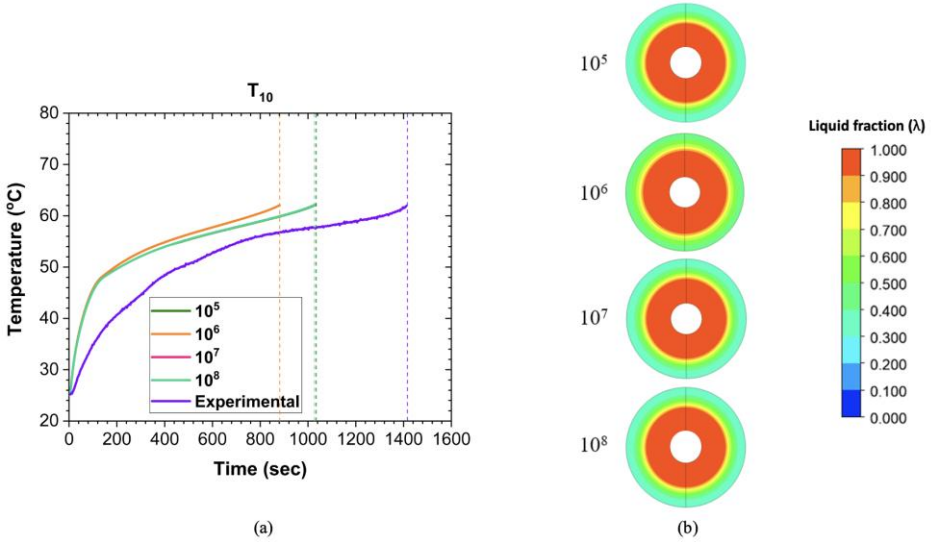

Figure 6. Local point temperature profiles at T_{10} in numerical and experimental studies (a), liquid fraction contours at t=600s (b) for varied mushy zone constants

Effect of Pressure-Velocity Coupling

In fluid dynamics simulations, pressure-velocity coupling refers to the whole set of methods used to ensure that the pressure and velocity fields are solved in a compatible with each other. This relationship plays a critical role in solving the Navier-Stokes equations, which are the equations of motion of the fluid. Since pressure and velocity cannot be solved independently, these two variables must be consistent with each other (Versteeg & Malalasekera, 2007; Tu et al., 2018). Otherwise, results of pressure and velocity distributions of the fluid may be incompatible with the fundamental principles of physics.

Figure 7 illustrates the T_{10} local point temperature profiles of various pressure-velocity relationship algorithms (Coupled, SIMPLE, SIMPLEC, PISO), alongside the findings of the experimental study, and the impact of these relationships on the melting process. It is possible to make the following definitions for the algorithm used in the analyses, respectively: The SIMPLE (Semi-Implicit Method for Pressure-Linked Equations) algorithm is a predictor-corrector method that is employed on a staggered numerical mesh. At each iteration step, the velocity and pressure fields are updated separately, and then linked with a pressure correction equation. It is the preferred option due to its straightforward implementation and minimal computational cost. The SIMPLE algorithm exhibits slow convergence in scenarios characterized by high Mach number flows (Versteeg & Malalasekera, 2007). This is not the case for the melting problem in the paraffin/graphite matrix composite structure, since the fluid is regarded as incompressible. The composite storage medium was observed to converge using the SIMPLE pressure-velocity coupling in 4150 iterations, with melting completed in 1027sec. The SIMPLEC (SIMPLE-Consistent) algorithm differs from SIMPLE in that it modifies the momentum equations in such a way that the velocity correction equations ignore less important terms than those used in SIMPLE. The improvements to the derivation of the pressure correction equation result in a more rapid convergence.

Furthermore, it requires a reduced number of iterations (ANSYS Inc, 2013). Nevertheless, it is complicated to apply to complex geometries and mesh structures. In this study, geometry is an annular geometry and since a structured mesh is used, the melting process was completed in 1031sec, exhibiting a rapid convergence (3200). It is clear from Figure 7 that the time-dependent thermal energy storage process reaches end point at the nearly same time as the SIMPLE and SIMPLEC algorithms. Although the PISO algorithm was originally developed to address time-dependent compressible flow problems without iteration, it has been successfully adapted to the iterative solution of steady-state problems. This algorithm requires extra memory as it solves the pressure correction term twice (Tu et al., 2018). For the PISO algorithm, which produces more accurate and stable results by using multiple pressure and velocity correction cycles at each time step, the paraffin/graphite matrix thermal energy storage process was completed in 1031sec. Although the PISO algorithm takes longer to converge than the SIMPLE (20.48%) and SIMPLEC (56.25%) algorithms, it should be noted that the time-dependent thermal energy storage process reaches its final at the same time as the SIMPLE and SIMPLEC algorithms. Finally, the Coupled algorithm means solving the pressure and velocity fields simultaneously. For the Coupled algorithm, which offers high accuracy solutions by providing a strong coupling between velocity and pressure, the paraffin/graphite matrix thermal energy storage process with a bulk density of 75 kg/m^3 completed the melting process in 1031sec. The correct implementation of SIMPLE, SIMPLEC, PISO and Coupled algorithms is a critical step for a successful CFD analysis.

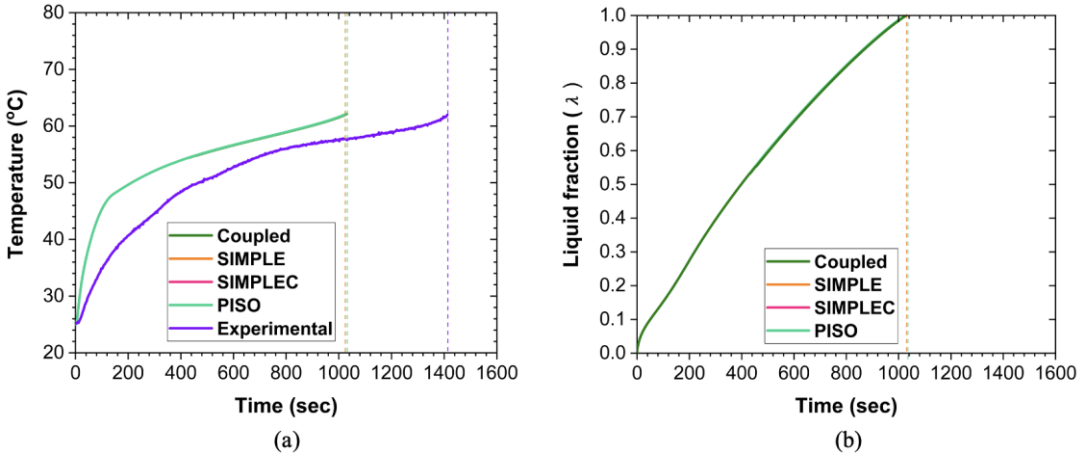

Figure 7. Effect of pressure-velocity coupling on T_{10} local point temperature profiles (a), liquid fractions (b)

Effect of Pressure Discretization Scheme

Pressure Discretization Scheme is used in fluid dynamics and heat transfer problems to discretize the pressure by determining the pressure distribution between nodes thereby allowing the solution of the momentum equations. The pressure discretization schemes implemented in this study are PRESTO! (Pressure Staggering Option) and Body Force Weighted, respectively. The following definitions can be made for these expressions, respectively: The PRESTO! scheme employs the discretized continuity equation (ANSYS Inc, 2013) to calculate the pressure on the surfaces of an arrayed control volume. This scheme is particularly important for problems where rotating flows and gravitational forces are important. In this study, the PRESTO! discretization approach is considered as an evaluation criterion due to the fact that the paraffin/graphite matrix composite thermal energy storage medium is modeled in a gravitational medium. On the other hand, the Body Force Weighted scheme calculates the pressure on the surfaces of each control volume on the assumption that the normal gradient of the difference between pressure and mass forces is constant (Tu et al., 2018). This scheme is especially preferred in cases where mass forces (gravity, electric field, magnetic field, etc.) are important. Figure 8 illustrates the impact of pressure discretization schemes on T_{10} local point temperature profiles in paraffin/graphite matrix

composite storage media. It becomes evident that the two schemes exhibit no significant discrepancy. However, it is observed that the melting process is completed at the 978sec under the influence of the Body Force Weighted scheme, while the melting is ended at the 1031sec in the PRESTO! discretization scheme (Figure 8-(b)). Compared to the experimental case where melting is completed in 1410sec, it can be observed that the PRESTO! discretization scheme provides results that are more closely aligned with reality, particularly in porous media flows where graphite matrix is used. It is indicated that the selection of an appropriate discretization scheme in numerical fluid dynamics simulations has a considerable impact on the nature of the problem and the accuracy of the solution.

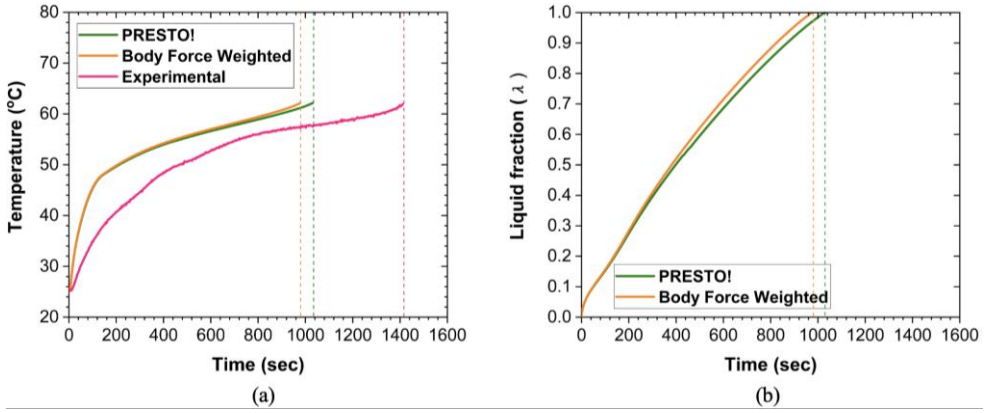

Figure 8. Effect of pressure discretization scheme on T10 local temperature profiles (a), liquid fractions (b)

Effect of Boundary Condition

The performance of thermal energy storage (TES) systems is significantly affected by the boundary conditions and the materials used for storage. The boundary conditions employed play an important role in energy storage and recovery processes, because it determines the thermal behavior of the storage system. The experimental study was conducted in ambient temperature of 25°C by insulating the storage medium. Nevertheless, it is not feasible to achieve a completely adiabatic wall, even with the implementation of an insulation layer into the system. Therefore, in order to observe whether the convection heat transfer coefficient has a significant effect on the experimental study during the phase change modelling, in addition to the adiabatic case study, a further analysis was conducted on the convection heat transfer to the ambient environment in the still air. A convective heat transfer boundary condition of 3 W/m^2K was applied to the outer wall of the storage medium geometry. Figure 9 illustrates the impact of the boundary condition on the melting process through the time-dependent T_{10} local point temperature profiles and melting times. Although the convection heat transfer coefficient does not have a significant difference on the temperature profile compared to the adiabatic case, it is observed that it improves the melting times by 53sec (Figure 9-(b)). The thermal energy storage/melting process is completed in 1031sec with convection heat transfer applied to the outer wall, while it is completed in 978sec for the adiabatic case. This is the result of an increase in thermal losses to the surrounding environment during the thermal energy storage/melting period. The temperature profiles obtained from the experimental study and numerical simulations exhibit similar characteristics. It should be noted that for the paraffin/graphite matrix configuration the discrepancies between the experimental and numerical outcomes are primarily attributable to inaccuracies in the measurement of thermophysical properties (due to instrumentation, human, and other factors). In addition, the assumption that material properties remain constant during numerical modelling, but in reality the composite material properties exhibit thermophysical (temperature-dependent) changes is another reasons. These factors significantly contribute to the development of present differences.

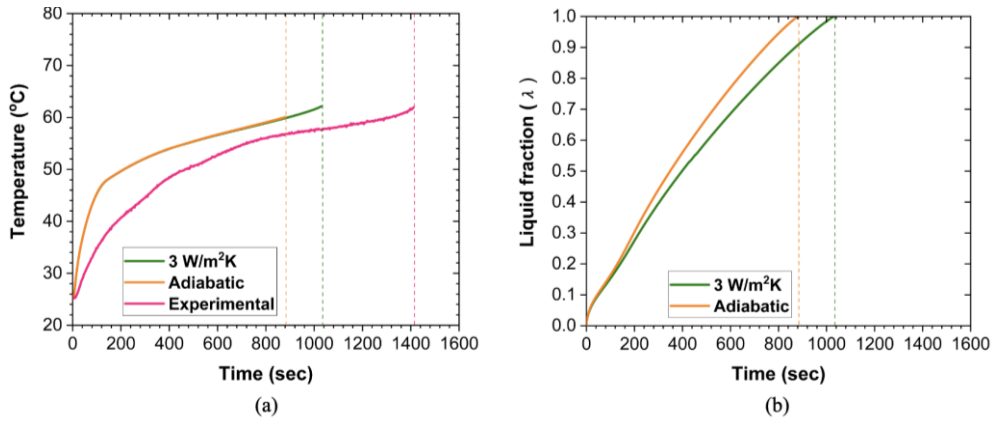

Figure 9. Effect of boundary condition on T_{10} local point temperature profile (a), liquid fraction (b)

Performance Assessment of Heat Storage Media

In the thermal energy storage medium with a bulk density value of 75 kg/m^3 and an isothermal wall boundary condition, the heat storage performance evaluation is based on the energy storage rate (S) for each case.

The following equations were utilized to assess storage performance:

$$S = \frac{Q_{total}}{m \times t} \tag{10}$$

Where Q_{total}, m, t are the amount of stored energy (J), mass (kg) and melting time (sec), respectively. Q_{total} is represented as follows:

$$Q_{total} = mC_{p,s}(T_m - T_i) + mL + mC_{p,l}(T_l - T_m)\ (J) \tag{11}$$

Here, m, $c_{p,s}$, L, $c_{p,l}$, T_m, T_i, T_l, represent mass (kg), specific heat in solid phase (J/kg.K), latent heat (J/kg), specific heat in liquid phase (J/kg.K), melting temperature (°C), initial temperature (°C) and final temperature of the composite (°C), respectively. Figure 10 illustrates the energy storage rates for all cases (both numerical and experimental) for the storage medium with a bulk density of 75 kg/m^3. This ratio varies with the parameters employed in the numerical studies. The main factor influencing the energy storage rate is the duration of the melting process and, consequently, the temperature variation in the final state of the system. It should be noted that the storage medium mass with a bulk density of 75 kg/m^3, along with its specific heat and latent heat are constant. To illustrate, the storage rates (S) for a range of constant mushy zones are as follows: 209.7, 245.5, 210.6 and 210.6 for 10^5, 10^6, 10^7 and 10^8, respectively. For the mushy constant of 10^6, there is a 17% increase in energy storage rate compared to 10^5. It results from an increase in storage times and a decrease in the final system temperature. Furthermore, the maximum energy storage rate achieved for the constant of 10^6 among all of the mushy zone variables. Among the pressure-velocity coupling schemes, the Coupled algorithm exhibits a 0.4% decrease in melting time in comparison to the other pressure-velocity algorithms. Moreover, it is concluded that the Body Force Weighted scheme exhibited the most optimal storage rate (221.1), particularly in storage mediums where the gravitational mass force is significant. In addition, an increase of 2.4% in the stored energy ratio was observed in the adiabatic case, wherein no heat transfer occurs from the storage medium to the surrounding environment, in comparison to the convection boundary condition. This phenomenon can be explained by the decrease in thermal energy storage/melting times and varied final TES system temperatures.

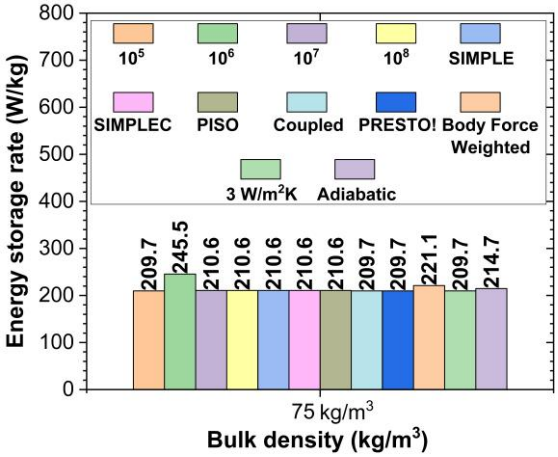

Figure 10. Energy storage rates of storage media with a bulk density of 75kg/m3 for various numerical approaches and experimental study

CONCLUSION

In this study, CFD simulations of a high thermal conductivity (7 W/mK) storage medium consisting of a paraffin-impregnated graphite matrix with a bulk density of 75 kg/m^3 were performed for the LHTES system. In the simulations, the numerical variables were analyzed through the mushy zone parameter (10^5, 10^6, 10^7, 10^8), the pressure-velocity coupling (SIMPLE, SIMPLEC, PISO, Coupled), the pressure discretization scheme (PRESTO!, Body Force Weighted) and the boundary condition (isothermal wall, adiabatic wall). Future studies may consider the temperature-dependent variations in the thermophysical properties of materials. Modeling can be conducted using the Volume of Fluid (VOF) approach, which accounts for volumetric expansion, or through specific heat capacity methods that utilize temperature-based approaches instead of enthalpy. In addition, the analysis of discharging period can be explored by expanding the effects of numerical variables.

The following results were obtained:

The conduction network enhanced by embedding expanded graphite material in paraffin as a thermal conductivity improvement material result in a uniform temperature field by providing a homogeneous temperature distribution in the composite structure.

Numerical variable effect for the paraffin-impregnated graphite matrix storage medium is not significant, considering a large-scale agreement between the numerical models and the experimental output. To illustrate, the shortest melting time was 881sec (10^6), while the longest melting time was 1031sec (10^5) for the mushy zone constant.

The PRESTO! discretization scheme yielded the most accurate results in terms of the T_{10} local point temperature profile and liquid fractions, with a deviation of only 16sec from the experimental results.

Although the melting times improved by 53s compared to the adiabatic case, the 3W/m²K convection boundary condition was found to more accurately captured the real condition of the process.

The numerical model that most closely approximates the experimental/real conditions is 10^5, which employs a constant mushy zone, a Coupled algorithm for the pressure-velocity coupling, PRESTO! for the pressure discretization scheme, and a 3W/m²K convection boundary condition.

Variations in energy storage rates are attributed to the changes in the numerical parameter, resulting in an increase or decrease in melting times and the final temperature readings of the TES system. Maximum storage rate of the TES system was achieved by 10^6 mushy zone constant.

ACKNOWLEDGEMENTS

We would like to thank TÜBİTAK for its support under the 2209-B University Students Industrial Research Projects Support Program with Project number 1139B412300550.

Conflict of Interest

The article authors declare that there is no conflict of interest between them.

Author's Contributions

Celal Mert DİKMETAŞ: Software, Validation, Investigation. Sare MITINCIK: Methodology, Software, Visualization, Writing. Ahmet AKTÜRK: Writing - Review & Editing. Mustafa Yusuf YAZICI: Conceptualization, Methodology, Supervision, Project administration.

REFERENCES

ANSYS Inc. (2013). Ansys Fluent Tutorial Guide. https://www.slideshare.net/slideshow/ansys-fluent-tutorial-guide-r-15/45961740 (Accessed: November 9, 2024)

Brent, A. D., Voller, V. R., & Reid, K. J. (1988). Enthalpy-porosity technique for modeling convection-diffusion phase change: Application to the melting of a pure metal. International Journal of Numerical Methods for Heat and Fluid Flow. https://doi.org/10.1080/10407788808913615

Buonomo, B., Celik, H., Ercole, D., Manca, O., & Mobedi, M. (2019). Numerical study on latent thermal energy storage systems with aluminum foam in local thermal equilibrium. Applied Thermal Engineering, 159. https://doi.org/10.1016/j.applthermaleng.2019.113980

Cai, Y., Zhang, N., Yuan, Y., Zhong, W., & Yu, N. (2021). Multi-energy driven form-stable phase change materials based on SEBS and reduced graphene oxide aerogel. Solar Energy Materials and Solar Cells, 233, 111390. https://doi.org/10.1016/j.solmat.2021.111390

Cano, D., Funéz, C., Rodriguez, L., Valverde, J. L., & Sanchez-Silva, L. (2016). Experimental investigation of a thermal storage system using phase change materials. Applied Thermal Engineering, 107, 264–270. https://doi.org/10.1016/j.applthermaleng.2016.06.169

Chakraborty, A., Noh, J., Mach, R., Shamberger, P., & Yu, C. (2022). Thermal energy storage composites with preformed expanded graphite matrix and paraffin wax for long-term cycling stability and tailored thermal properties. Journal of Energy Storage, 52, 104856. https://doi.org/10.1016/j.est.2022.104856

Chinnasamy, V., Heo, J., Jung, S., Lee, H., & Cho, H. (2023). Shape stabilized phase change materials based on different support structures for thermal energy storage applications–A review. Energy, 262, 125463. https://doi.org/10.1016/j.energy.2022.125463

Dinçer, I., & Rosen, M. A (2002). Thermal Energy Storage Systems and applications. John Wiley & Sons, Inc.

Elakkiyadasan, R., Gavaskar, T., Murugapoopathi, S., Sathishkumar, N., Nagaraja, M., & Ganesh, K. (2022). Experimental investigation of PCM with added E-graphite and analysis of its thermal characteristics. Materials Today: Proceedings, 64, 1717–1720.https://doi.org/10.1016/j.matpr.2022.05.493

Feng, Z., Li, Y., He, F., Li, Y., Zhou, Y., Yang, Z., He, R., Zhang, K., & Yang, W. (2020). Experimental and numerical simulation of phase change process for paraffin in three-dimensional graphene aerogel. Applied Thermal Engineering, 167. https://doi.org/10.1016/j.applthermaleng.2019.114773

Fteiti, M., & Alaidrous, A. (2020). Latent heat storage during melting and solidification of a phase change material (PCM) embedded with a porous matrix of high thermal conductivity. International Journal of Energy Engineering, 2020, 1–9. https://doi.org/10.5923/j.ijee.20201001.01

Kang, S., Choi, J. Y., & Choi, S. (2019). Mechanism of heat transfer through porous media of inorganic intumescent coating in cone calorimeter testing. Polymers, 11(2), 221. https://doi.org/10.3390/polym11020221

Khatibi, M., Nemati-Farouji, R., Taheri, A., Kazemian, A., Ma, T., & Niazmand, H. (2021). Optimization and performance investigation of the solidification behavior of nano-enhanced phase change materials in triplex-tube and shell-and-tube energy storage units. Journal of Energy Storage, 33. https://doi.org/10.1016/j.est.2020.102055

Kumar, N., Shrivastava, A., & Chakraborty, P. R. (2024). Enhancing latent heat storage dynamics with expanded graphite foam: Myth vs. reality check through numerical and experimental investigations. Available at SSRN, http://dx.doi.org/10.2139/ssrn.4867508

Li, C., Li, Q., & Ge, R. (2022). Enhancement of melting performance in a shell and tube thermal energy storage device under different structures and materials. Applied Thermal Engineering, 214. https://doi.org/10.1016/j.applthermaleng.2022.118701

Ling, Z., Chen, J., Xu, T., Fang, X., Gao, X., & Zhang, Z. (2015). Thermal conductivity of an organic phase change material/expanded graphite composite across the phase change temperature range and a novel thermal conductivity model. Energy Conversion and Management, 102, 202–208. https://doi.org/10.1016/j.enconman.2014.11.040

Liu, W., Bie, Y., Xu, T., Cichon, A., Królczyk, G., & Li, Z. (2022). Heat transfer enhancement of latent heat thermal energy storage in solar heating system: A state-of-the-art review. Journal of Energy Storage, 46. https://doi.org/10.1016/j.est.2021.103727

Mhiri, H., Jemni, A., & Sammouda, H. (2020). Numerical and experimental investigations of melting process of composite material (nanoPCM/carbon foam) used for thermal energy storage. Journal of Energy Storage, 29, 101167. https://doi.org/10.1016/j.est.2019.101167

Mitali, J., Dhinakaran, S., & Mohamad, A. A. (2022). Energy storage systems: a review. Energy Storage and Savings, 1, 166–216. https://doi.org/10.1016/j.enss.2022.07.002

Mitincik, S., & Yazici, M. Y. (2023). Numerical study on the thermal energy storage performance of graphite matrix composite with phase change in shell-in-tube: Effects of bulk density and wall temperature. Journal of Energy Storage, 72, 108304. https://doi.org/10.1016/j.est.2023.108304

Mitincik, S., & Yazici, M. Y. (2024). Numerical modelling and experimental validation on the discharging performance of paraffin/graphite matrix composite with various configurations of bulk density and wall temperature. Journal of Energy Storage, 89, 111704. https://doi.org/10.1016/j.est.2024.111704

Muraleedharan Nair, A., Wilson, C., Kamkari, B., Locke, J., Jun Huang, M., Griffiths, P., & Hewitt, N. J. (2024). Advancing thermal performance in PCM-Based energy Storage: A comparative study with Fins, expanded Graphite, and combined configurations. Energy Conversion and Management: X, 23(May), 100627. https://doi.org/10.1016/j.ecmx.2024.100627

Nair, A. M., Wilson, C., Huang, M. J., Griffiths, P., Hewitt, N., Singh, D., Buddhi, D., & Karthick, A. (2023). Phase change materials in building integrated space heating and domestic hot water applications: A review. Environmental Science and Pollution Research, 54(May), 44–77. https://doi.org/10.1016/j.est.2022.105227

Opolot, M., Zhao, C., Liu, M., Mancin, S., Bruno, F., & Hooman, K. (2020). Influence of cascaded graphite foams on thermal performance of high temperature phase change material storage systems. Applied Thermal Engineering, 180, 115618. https://doi.org/10.1016/j.applthermaleng.2020.115618

Pourakabar, A., & Rabienataj Darzi, A. A. (2019). Enhancement of phase change rate of PCM in cylindrical thermal energy storage. Applied Thermal Engineering, 150, 132–142. https://doi.org/10.1016/j.applthermaleng.2019.01.009

Singh, D., Buddhi, D., & Karthick, A. (2023). Productivity enhancement of solar still through heat transfer enhancement techniques in latent heat storage system: a review. Environmental Science and Pollution Research, 30(1), 44–77. https://doi.org/10.1007/s11356-022-23964

Song, Y., Zhang, N., Jing, Y., Cao, X., Yuan, Y., & Haghighat, F. (2019). Experimental and numerical investigation on dodecane/expanded graphite shape-stabilized phase change material for cold energy storage. Energy, 189.https://doi.org/10.1016/j.energy.2019.116175

Tong, X., Li, N., Zeng, M., & Wang, Q. (2019). Organic phase change materials confined in carbon-based materials for thermal properties enhancement: Recent advancement and challenges. Renewable and Sustainable Energy Reviews, 108, 398–422. https://doi.org/10.1016/j.rser.2019.03.031

Tu, J., Yeoh, G. H., & Liu, C. (2018). Computational Fluid Dynamics: A practical approach. Butterworth-Heinemann.

Versteeg, H. K., & Malalasekra, W. (2007). An introduction to computational fluid dynamics: The Finite Volume Method. Pearson.

Voller, V. R., & Prakash, C. (1987). A fixed grid numerical modelling methodology for convection-diffusion mushy region phase-change problems. International Journal of Heat and Mass Transfer, 30, 1709–1719. https://doi.org/10.1016/0017-9310(87)90317-6

Wu, S., Yan, T., Kuai, Z., & Pan, W. (2020). Experimental and numerical study of modified expanded graphite/hydrated salt phase change material for solar energy storage. Solar Energy, 205, 474–486. https://doi.org/10.1016/j.solener.2020.05.052

Yazici, M. Y. (2022). The effect of a new design preheating unit integrated to graphite matrix composite with phase change battery thermal management in low-temperature environment: An experimental study. Thermal Science and Engineering Progress, 29, 101244. https://doi.org/10.1016/j.tsep.2022.101244

Yazici, M. Y., Saglam, M., Aydin, O., & Avci, M. (2021). Thermal energy storage performance of PCM/graphite matrix composite in a tube-in-shell geometry. Thermal Science and Engineering Progress, 23. https://doi.org/10.1016/j.tsep.2021.100915

Zhao, B., Li, C., Jin, Y., Yang, C., Leng, G., Cao, H., Li, Y., & Ding, Y. (2016). Heat transfer performance of thermal energy storage components containing composite phase change materials. IET Renewable Power Generation, 10, 1515–1522. https://doi.org/10.1049/iet-rpg.2016.0026

Zhao, C., Opolot, M., Liu, M., Bruno, F., Mancin, S., & Hooman, K. (2021). Phase change behaviour study of PCM tanks partially filled with graphite foam. Applied Thermal Engineering, 196, 117313. https://doi.org/10.1016/j.applthermaleng.2021.117313